

Dynamic buckling of thin thermoviscoplastic cylindrical shell under radial impulsive loading

Z.G. Wei, R.C. Batra*

Department of Engineering Science and Mechanics, MC 0219, Virginia Polytechnic Institute and State University, Blacksburg, VA 24061, USA

Received 29 March 2006; received in revised form 15 September 2006; accepted 12 October 2006

Available online 1 December 2006

Abstract

The dynamic plastic buckling of a homogeneous and isotropic thin thermoviscoplastic cylindrical shell loaded radially is studied analytically by analyzing the stability of its stressed/deformed configuration under superimposed infinitesimal perturbations. The wave number of the perturbation that maximizes its initial growth rate is assumed to determine the buckling mode. Cubic algebraic equations are obtained for both the maximum initial growth rate of perturbation and the corresponding wave number. The buckled shape of a cylindrical shell is found to match well with that observed experimentally. The sensitivity of the buckled shape to the impact velocity, the hardening modulus, and the material viscosity has been delineated. For axially restrained shells, it is found that for materials exhibiting strain rate hardening only the maximum initial growth rate of the perturbation and the corresponding wave number vary as $(\bar{\sigma}^0/\rho\beta)^{1/3}h^{-2/3}$ and $(\rho/\bar{\sigma}^0)^{1/6}R\beta^{-1/3}h^{-2/3}$, respectively. For axially unrestrained cylindrical shells made of strain hardening only materials, the maximum initial growth rate of a perturbation and the corresponding wave number vary as $(\bar{\sigma}^0/h)(\rho E)^{-1/2}$ and $(R/h(\bar{\sigma}^0/E))^{1/2}$, respectively. Here $\bar{\sigma}^0$ is the mean value of the generalized stress, ρ the mass density, β the material viscosity, h the shell thickness, and R the mean radius of the shell.

© 2006 Elsevier Ltd. All rights reserved.

Keywords: Instability; Buckling; Cylindrical shell; Radial impulsive loading

1. Introduction

Dynamic buckling is an important design consideration for thin-walled metallic cylindrical, spherical, and conical shells likely to be subjected to explosive loads that have significant radial components. For example, explosive devices are used for rapidly closing pipes, as shaped-charge weapons, and as oil well perforators. In order to work effectively, shaped charge liners should collapse without buckling and wrinkling. There are numerous works on buckling of rings and cylindrical shells subjected to radial impulsive loads. Depending on the radius-to-thickness ratio of the ring or the shell and its material, the buckling can be either elastic or plastic. The transition from elastic to plastic flow buckling occurs at a radius-to-thickness ratio of about 200 for most engineering metals [1].

Axial crushing of thin-walled shells under quasi-static and dynamic loads has also been studied [2]. Several papers are available on the plastic buckling of cylindrical shells subjected to impulsive pressure loads, e.g. see the review paper by Jones and Okawa [3].

A commonly adopted dynamic buckling criterion is due to Abrahamson and Goodier [4], who introduced the concept of amplification function, which is the ratio of the maximum amplitude of shape imperfection associated with the n th mode to its initial value. The structure is taken to have buckled when the amplification function exceeds a prespecified value (e.g. 10, 100, 1000, ...). This criterion has been successfully used to analyze the plastic buckling of rods due to axial impact [5], plastic buckling of plates due to in-plane forces [6], and plastic buckling of cylinders under axial impact [7].

There are several works on the radial buckling of cylindrical shells under impulsive loading. For example, Goodier and McIvor [8] studied the buckling of cylindrical elastic shells under uniform radial impulse with small initial

*Corresponding author. Tel.: +1 540 231 6051; fax: +1 540 231 4574.
E-mail address: rbatra@vt.edu (R.C. Batra).

velocity. Lindberg [9] found the buckling transition from vibrating buckling to pulse buckling for intermediate initial velocities. Pulse buckling can be found at higher initial velocities [10]. Radial plastic buckling of cylindrical shells has been studied in Refs. [11,12]. Wang and Ru [13] used the following energy criterion to analyze dynamic buckling of cylinders under impulsive loads: the structure is stable if under a kinematically admissible perturbation imposed on its dominant motion, the energy required to deform the structure due to the perturbation is greater than or equal to the work done by external forces. The instability of the structure is taken to be synonymous with its buckling. The energy criterion has been successfully applied to the radial buckling of cylindrical shells by Gu et al. [14]. Batra and Wei [15] hypothesized that the deformed state of a structure is unstable if infinitesimal disturbances superimposed upon it begin to grow, and the wave number of the perturbation corresponding to the maximum initial growth rate gives the buckling mode of the structure. They used this criterion to study the instability of a thin thermoviscoplastic plate. Wei et al. [16] used the same criterion to analyze buckling of a thin thermoviscoplastic cylindrical shell under axial impact. This method has also been used to delineate spacing among adjacent adiabatic shear bands in thermoviscoplastic materials [17].

Here we use the perturbation method to analyze plastic buckling of thin cylindrical shells under radial impulsive loading. A closed form expression for the wave number of the buckled cylinder has been derived, and scaling laws stated in the abstract have been deduced.

2. Dynamic plastic buckling analyzed by the perturbation method

2.1. Formulation of the problem

The dynamic elastic–plastic buckling of structures is a complex phenomenon due to various factors such as inertia effects, large deformations, and inelastic behavior. It is thus not possible to solve the problem analytically, and simplified models are necessary to deduce general trends. Fig. 1 shows a schematic sketch of the problem studied. Following [1], it is assumed that the shell is radially loaded with a uniform prescribed velocity, elastic deformations are negligible, plastic deformations are isochoric, perturbations are infinitesimal so that no strain-rate reversal occurs until the buckling modes have well developed, and the material of the shell is isotropic, homogeneous, obeys von Mises yield criterion, and exhibits isotropic strain and strain-rate hardening and thermal softening. In [1] the preferred buckling mode is determined numerically by the amplification of initial imperfection for linear hardening materials. Here closed form expressions for the growth rate of perturbation and the wave number that maximizes it are derived for linear viscoplastic materials. From these buckling modes can be easily found.

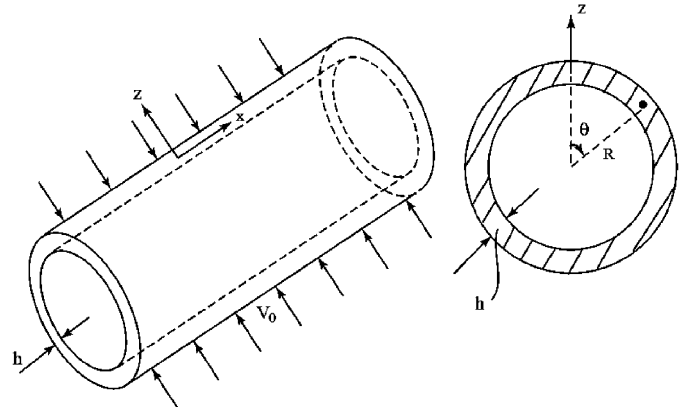


Fig. 1. Schematic sketch of the problem studied, and the side view of a cross-section.

It has been observed experimentally that imploded cylindrical shells remain straight except in a narrow region near each end where the shell flares outwards slightly. Consequently, it is assumed here that the axial strain is constant through the shell thickness, i.e., it is independent of the thickness coordinate z . It has also been observed that, even in a severely buckled shell, plane sections perpendicular to the shell axis remain plane; thus the axial strain is taken to be independent of the angular position θ of a point.

For a thin shell, it is reasonable to assume that the stress component perpendicular to the mid-surface of the shell is negligible, i.e., $\sigma_z = 0$. Assuming that sides of shell elements formed by planes perpendicular to the shell axis remain plane during longitudinal bending, we apply the radial load N_z to create a uniform stress field σ_x, σ_θ and the strain-rate field $\dot{\epsilon}_x, \dot{\epsilon}_\theta$. Let the total inward radial displacement be $w(x, t)$. Then the circumferential strain rate is

$$\dot{\epsilon}_\theta = -\left(1 - \frac{z}{R}\right) \frac{\dot{w}_0}{R} + \left(\frac{z}{R}\right) \frac{1}{R} \dot{w}'' \tag{1}$$

and the axial strain rate, unaffected by perturbations, is given by

$$\dot{\epsilon}_x = -k\dot{\epsilon}_\theta = k(x) \frac{\dot{w}_0}{R}, \quad 0 \leq k \leq 1/2, \quad z = 0, \tag{2}$$

where $\dot{w}_0 = V_0$ is the radial impact velocity, R equals the mean radius of the shell, k is a measure of the axial restraint, and a superimposed dot and a prime denote, respectively, the partial differentiation with respect to time t and the angular position θ . $\dot{\epsilon}_{x0}, \dot{\epsilon}_{\theta0}$, are the longitudinal and the circumferential strain rate components on the midsurface of the shell. $k = 0$ represents complete constraint in the axial direction, and $k = 1/2$ no restraint.

The incompressibility condition is

$$\dot{\epsilon}_x + \dot{\epsilon}_\theta + \dot{\epsilon}_z = 0. \tag{3}$$

The effective strain rate is given by [1]

$$\dot{\epsilon}^2 = \frac{2}{3} (\dot{\epsilon}_x^2 + \dot{\epsilon}_\theta^2 + \dot{\epsilon}_z^2). \tag{4}$$

The axial and the hoop stress components derived from the flow rule associated with the von Mises yield criterion can be written as

$$\sigma_x = \frac{2(2\dot{\epsilon}_x + \dot{\epsilon}_\theta)\sigma}{3\dot{\epsilon}}, \quad \sigma_\theta = \frac{2(2\dot{\epsilon}_\theta + \dot{\epsilon}_x)\sigma}{3\dot{\epsilon}}, \quad (5)$$

where σ is the effective stress.

We assume that the strain hardening, strain rate hardening, and thermal softening of the material can be approximately by

$$\sigma = \sigma_0(1 + \bar{\alpha}\epsilon)(1 + \beta\dot{\epsilon})(1 - \gamma\theta) \quad (6)$$

which follows from the Litonski–Batra thermoviscoplastic relation [18]

$$\sigma = \sigma_0 \left(1 + \frac{\epsilon}{\epsilon_y}\right)^n (1 + B\dot{\epsilon})^m (1 - \gamma\theta), \quad (7)$$

when $m = n = 1$. For many engineering materials the addition to the flow stress due to work hardening, strain-rate hardening, and thermal softening terms is small as compared to the quasistatic yield stress of the material, and Eq. (6) can be approximated by

$$\sigma = \sigma_0[1 + \bar{\alpha}\epsilon + \beta\dot{\epsilon} - \gamma\theta]. \quad (8)$$

If the part χ of the plastic work is converted into heat and effects of heat conduction can be neglected, then the temperature rise θ can be estimated by $\chi\sigma\epsilon/\rho c$ where ρ is the mass density and c the specific heat. Substitution for θ into Eq. (8) and setting $\alpha = \bar{\alpha} - \gamma\chi\sigma\epsilon/\rho c$, we get

$$\sigma = \sigma_0[1 + \alpha\epsilon + \beta\dot{\epsilon}], \quad (9)$$

where α and β are the effective strain hardening and the strain rate hardening coefficients, respectively. χ is usually in the range of 0.85–0.95 for metals. Note that α depends upon σ and ϵ . Since the buckling mode is determined during early stages of deformation the temperature rise is not significant and one can take $\alpha = \bar{\alpha}$.

Henceforth, terms with powers of z/R higher than one and terms involving products of displacement will be neglected. In order to simplify expressions, we set

$$K_1 = 2(1 - k + k^2), \quad K_2 = (3K_1/2)^{1/2}, \quad K_3 = (2 - k)/K_1 \quad (10)$$

Thus, by substituting from Eqs. (1)–(3) into Eq. (4), we get the following expression for the generalized strain rate.

$$\dot{\epsilon} = \frac{2K_2}{3} \left(\frac{\dot{w}_0}{R} - \frac{z}{R} K_3 \frac{1}{R} (\dot{w}_0 + \dot{w}'') \right). \quad (11)$$

The integration of Eq. (11) with respect to time gives

$$\epsilon = \frac{2K_2}{3} \left(\frac{w_0}{R} - \frac{z}{R} K_3 \frac{1}{R} (w_0 + w'') \right). \quad (12)$$

Eq. (12) is a little different from that obtained by Lindberg and Florence [1] because they considered the effect of initial imperfections, and we have assumed there are no initial defects.

Substitution from Eqs. (11) and (12) into Eq. (9) gives the following expression for the generalized

stress:

$$\sigma = \sigma^0 - \left(\frac{z}{R}\right) \frac{2K_2 K_3 \sigma_0}{3R} [\alpha(w_0 + w'') + \beta(\dot{w}_0 + \dot{w}'')], \quad (13)$$

where $\sigma^0 = \sigma_0[1 + (2K_2/3R)(\alpha w_0 + \beta \dot{w}_0)]$ is the generalized stress at the mid-surface of the shell. Stress components derived from Eqs. (1), (2), (9), (11) and (5), have the following expressions:

$$\begin{aligned} \sigma_x &= -\frac{(1-2k)\sigma^0}{K_2} + \left(\frac{z}{R}\right) \frac{1}{K_2} \left\{ \sigma^0 \left(1 + \frac{\dot{w}''}{\dot{w}_0}\right) \right. \\ &\quad \times [(2k-1)K_3 + 1] \\ &\quad \left. - \frac{2(2k-1)K_2 K_3 \sigma_0 \dot{w}_0}{3R} \left[\alpha \frac{(w_0 + w'')}{\dot{w}_0} + \beta \left(1 + \frac{\dot{w}''}{\dot{w}_0}\right) \right] \right\} \\ \sigma_\theta &= -\frac{(1-2k)\sigma^0}{K_2} + \left(\frac{z}{R}\right) \frac{1}{K_2} \left\{ \sigma^0 \left(1 + \frac{\dot{w}''}{\dot{w}_0}\right) [(k-2)K_3 + 2] \right. \\ &\quad \left. - \frac{2(k-2)K_2 K_3 \sigma_0 \dot{w}_0}{3R} \left[\alpha \frac{(w_0 + w'')}{\dot{w}_0} + \beta \left(1 + \frac{\dot{w}''}{\dot{w}_0}\right) \right] \right\} \end{aligned} \quad (14)$$

Adopting the sign convention of [1], stresses have the following resultant forces and moments

$$\begin{aligned} N_x &= \int_{-h/2}^{h/2} \sigma_x dz = -\frac{(1-2k)h\bar{\sigma}^0}{K_2}, \\ N_\theta &= \int_{-h/2}^{h/2} \sigma_\theta dz = -\frac{(2-k)h\bar{\sigma}^0}{K_2}, \end{aligned} \quad (15)$$

$$\begin{aligned} M_x &= -\int_{-h/2}^{h/2} \sigma_x z dz \\ &= \frac{h^3}{12RK_2} \left\{ \bar{\sigma}^0 \left(1 + \frac{\dot{w}''}{\dot{w}_0}\right) [(2k-1)K_3 + 1] \right. \\ &\quad \left. - \frac{2(2k-1)K_2 K_3 \sigma_0 \dot{w}_0}{3R} \left[\alpha \frac{(w_0 + w'')}{\dot{w}_0} + \beta \left(1 + \frac{\dot{w}''}{\dot{w}_0}\right) \right] \right\}, \\ M_\theta &= -\int_{-h/2}^{h/2} \sigma_\theta z dz \\ &= \frac{h^3}{12RK_2} \left\{ \bar{\sigma}^0 \left(1 + \frac{\dot{w}''}{\dot{w}_0}\right) [(k-2)K_3 + 2] \right. \\ &\quad \left. - \frac{2(k-2)K_2 K_3 \bar{\sigma}_0 \dot{w}_0}{3R} \left[\alpha \frac{(w_0 + w'')}{\dot{w}_0} + \beta \left(1 + \frac{\dot{w}''}{\dot{w}_0}\right) \right] \right\}, \end{aligned} \quad (16)$$

where h is the thickness of the shell. We have replaced the generalized stress at the mid-surface by its mean value $\bar{\sigma}^0$ as was done in [1].

The transverse motion of a cylindrical shell is governed by [1]

$$M_\theta'' - N_\theta w'' + \rho h R^2 \ddot{w} = 0. \quad (17)$$

After substituting from Eqs. (15)₂ and (16)₂ for forces and moments into Eq. (17), we arrive at

$$\ddot{w} + a w'' + b \ddot{w}'' + c w'''' = 0, \quad (18)$$

where

$$\begin{aligned}
 a &= \frac{(2-k)\bar{\sigma}^0}{\rho R^2 K_2}, \\
 b &= \frac{h^2}{12\rho R^3 K_2} \left\{ \frac{3R[K_3(k-2) + 2]\bar{\sigma}^0 + 2K_2 K_3(2-k)\beta\bar{\sigma}_0}{3R\dot{w}_0} \right\}, \\
 c &= \frac{K_3(2-k)\alpha\bar{\sigma}_0 h^2}{18\rho R^4}.
 \end{aligned} \tag{19}$$

For materials exhibiting strain hardening only, $\beta = 0$, then

$$\begin{aligned}
 a &= \frac{(2-k)\bar{\sigma}^0}{\rho R^2 K_2}, \quad b = \frac{K_3 k^2 h^2 \bar{\sigma}^0}{4\rho(2-k)K_2 R^3 \dot{w}_0}, \\
 c &= \frac{K_3(2-k)\alpha\bar{\sigma}_0 h^2}{18\rho R^4}.
 \end{aligned} \tag{20}$$

For materials exhibiting strain rate hardening only, $\alpha = 0$, then

$$a = \frac{(2-k)\bar{\sigma}^0}{\rho R^2 K_2}, \quad b = \frac{h^2 \bar{\sigma}_0}{12\rho R^3} \left(\frac{3k^2}{K_1 K_2 \dot{w}_0} + \frac{4\beta}{3R} \right). \tag{21}$$

3. Buckling criterion and buckled shapes

In order to find the buckling mode we perturb the deformed state of the cylindrical shell by an infinitesimal amount. If the superimposed perturbations grow with time, then the deformation is unstable, we regard the shell to have buckled, and take its buckled shape to correspond to the wave number of the perturbation that has the maximum initial growth rate.

Let $w_0(x) = w(x, t_0)$ give the deflection of the shell at time $t = t_0$, and an infinitesimal perturbation $\delta w(x, t)$ where $|\delta w/w_0| \ll 1$ and $|\delta \dot{w}/\dot{w}_0| \ll 1$, be added to it. We assume that resultant forces and moments are unaffected by the superimposed perturbation. Furthermore, we set

$$\delta w(x, t) = \delta w^* e^{\eta(t-t_0)} \sin(\omega\theta). \tag{22}$$

In Eq. (22), η is the initial growth rate of the perturbation at time $t = t_0$, and ω the wave number. A positive value of η implies that the deformed shell at time t_0 has buckled. Substituting $w = w_0 + \delta w$ into Eq. (18), and subtracting Eq. (18) from the resulting equation, we get the following algebraic equation relating the wave number ω to the growth rate η .

$$\eta^2 - a\omega^2 + b\eta\omega^4 + c\omega^4 = 0. \tag{23}$$

In order to find the wave number that has the maximum initial growth rate we set

$$\frac{\partial \eta}{\partial \omega^2} = 0. \tag{24}$$

Eq. (24) gives

$$\eta = \frac{a - 2c\omega^2}{2b\omega^2} \quad \text{or} \quad \omega^2 = \frac{a}{2(b\eta + c)}. \tag{25}$$

Substituting from Eq. (25) into Eq. (23), we obtain the following two cubic algebraic equations for the growth rate and the wave number

$$\begin{aligned}
 \eta^3 + f_1\eta^2 + f_3 &= 0, \\
 \omega^6 + g_1\omega^4 + g_2\omega^2 + g_3 &= 0,
 \end{aligned} \tag{26}$$

where

$$\begin{aligned}
 f_1 &= \frac{c}{b}, \quad f_3 = -\frac{a^2}{4b}, \\
 g_1 &= -\frac{2c^2}{ab^2}, \quad g_2 = \frac{2c}{b^2}, \quad g_3 = -\frac{a}{2b^2}.
 \end{aligned}$$

The cubic Eq. (26) has either one real root and two complex conjugate roots, or three real roots of which at least two are equal, or three different real roots according as $(p_1/3)^3 + (q_1/2)^2$ and $(p_2/3)^3 + (q_2/2)^2$ are positive, zero, or negative, respectively. Here

$$\begin{aligned}
 p_1 &= -f_1^2/3, \quad q_1 = 2(f_1/3)^3 + f_3, \\
 p_2 &= -g_1^2/3 + g_2, \\
 q_2 &= 2(g_1/3)^3 - (g_1 g_2)/3 + g_3.
 \end{aligned}$$

If $(p_1/3)^3 + (q_1/2)^2 \geq 0$ and $(p_2/3)^3 + (q_2/2)^2 \geq 0$, then real roots of the cubic Eqs. (26) are

$$\begin{aligned}
 \eta &= \sqrt[3]{-q_1/2 + \sqrt{(p_1/3)^3 + (q_1/2)^2}} \\
 &\quad + \sqrt[3]{-q_1/2 - \sqrt{(p_1/3)^3 + (q_1/2)^2}} - f_1/3,
 \end{aligned} \tag{27}$$

$$\begin{aligned}
 \omega^2 &= \sqrt[3]{-q_2/2 + \sqrt{(p_2/3)^3 + (q_2/2)^2}} \\
 &\quad + \sqrt[3]{-q_2/2 - \sqrt{(p_2/3)^3 + (q_2/2)^2}} - g_1/3.
 \end{aligned} \tag{28}$$

If $(p_1/3)^3 + (q_1/2)^2 < 0$ and $(p_2/3)^3 + (q_2/2)^2 < 0$, then three real roots of the cubic equations are

$$\begin{aligned}
 \eta_1 &= 2\sqrt{-p_1/3} \cos(\xi/3), \\
 \eta_2, \eta_3 &= -2\sqrt{-p_1/3} \cos(\xi/3 \pm 60^\circ)
 \end{aligned} \tag{29}$$

where

$$\cos(\xi) = -q_1/2\sqrt{-(p_1/3)^3}$$

and

$$\begin{aligned}
 \omega_1^2 &= 2\sqrt{-p_2/3} \cos(\zeta/3), \\
 \omega_2^2, \omega_3^2 &= -2\sqrt{-p_2/3} \cos(\zeta/3 \pm 60^\circ),
 \end{aligned} \tag{30}$$

where $\cos(\zeta) = -(q_2/2\sqrt{-(p_2/3)^3})$.

For materials exhibiting strain rate hardening only, $\alpha = 0$ which implies that $f_1 = g_1 = g_2 = 0$. Thus $p_1 = 0$, $q_1 = f_3$, $p_2 = 0$, $q_2 = g_3$, and Eqs. (26) have the

solution

$$\eta = \left(\frac{a^2}{4b}\right)^{1/3},$$

$$\omega = \left(\frac{a}{2b^2}\right)^{1/6}. \tag{31}$$

Substituting from Eq. (21) into Eq. (31), and setting $k = 0$, we have a simple scaling law for an axially restrained cylindrical shell

$$\eta = 3^{1/3} \left(\frac{\bar{\sigma}^0}{\rho\beta}\right)^{1/3} h^{-2/3},$$

$$\omega = (27\sqrt{3})^{1/6} \left(\frac{\rho}{\sigma^0}\right)^{1/6} R\beta^{-1/3}(h)^{-2/3}. \tag{32}$$

Eq. (32) is very similar to Eq. (4.2.40) of [1]. However, Eq. (32) is valid only for $k = 0$, and Eq. (31) holds for $k \neq 0$.

It is clear from Eq. (32) that the maximum initial growth rate of the perturbation increases with an increase in the mean generalized stress, but decreases with an increase in the mass density, strain rate hardening coefficient, and the shell thickness. The corresponding wave number increases with an increase in the mass density, the radius of the shell, but decreases with an increase in the strain rate hardening coefficient, the shell thickness and the mean generalized stress. However, the influence of the mass density and the generalized stress on the wave number is insignificant due to the low value of the exponent.

For axially restrained shells made of materials exhibiting strain hardening only, we set $k = 0$, then $b = 0$, and get the following simple scaling law.

$$\eta = \frac{\sqrt{3\bar{\sigma}^0}}{h\sqrt{E\rho}},$$

$$\omega = \sqrt{3\sqrt{3}} \frac{R}{h} \sqrt{\frac{\bar{\sigma}^0}{E}}, \tag{33}$$

where $E = \alpha\sigma_0$ is the hardening modulus of the material. For these shells, the maximum initial growth rate of the perturbation increases with the stress level, but decreases with an increase in the mass density, strain hardening modulus and the shell thickness. The corresponding wave number increases with an increase in the radius of the shell and the generalized mean stress level, decreases with an increase in the strain hardening modulus and the shell thickness, but is independent of the mass density. Expressions in Eq. (33) coincide with those for the buckling of a rod, except for the coefficient of the wave number [5].

If we set $b = c = 0$ which, for example, will hold when $\alpha = \beta = k = 0$, then Eq. (23) give $\eta^2 = a\omega^2$. That is, the initial growth rate of a perturbation is proportional to its wave number.

3.1. Buckling modes

Even though buckling modes for a general linearly strain- and strain-rate hardening material have been derived, for comparison with experimental results available in the literature, strain hardening only and strain rate hardening only materials are considered separately.

3.1.1. Strain hardening only materials

The 6061-T6 aluminum alloy is assumed to be strain rate insensitive, and have the following values for its material parameters.

$$E_h = 2275 \text{ MPa}, \quad \bar{\sigma}^0 = 290 \text{ MPa}, \quad \rho = 2700 \text{ kg/m}^3,$$

$$V_0 = I/\rho h.$$

Here E_h is the hardening modulus, and I the initial impulse per unit surface area imparted to the cylinder. Values of other material and geometric parameters, and observed and computed buckling modes are listed in Table 1.

Numerical calculations reported in [1] show that both the amplitude and the velocity amplification spectra

Table 1
Computed and observed number of half waves for 6061-T6 aluminum cylindrical shells

Shell number	Number of shells	Radius R (cm)	Thickness h (cm)	Impulse I (Ns/m ²)	Velocity (m/s)	Strain rate (1/s)	$k = \epsilon_x/\epsilon_y$	Strain (%)	Half-waves n (Exp.) [1]	Half-waves n (Theo.) [1]	Half-waves n (Present model)
1	3	3.729	0.165	650	146	3915	0.48	9.5	15	13	14
	3			650	146	3915	0.42	9.2	15	14	15
	2			650	146	3915	0.28	8.6	16	16	17
	1			630	141	3781	0.09	8.4	19	22	18
	1			630	141	3781	0.03	8.3	20	19	18
2	3	3.706	0.211	660	116	3130	0.48	6.2	14	11	11
	3			660	116	3130	0.42	6.0	15	12	12
	2			660	116	3130	0.28	5.6	15	14	13
3	3	3.691	0.241	690	106	2872	0.48	5.2	11	10	10
	3			690	106	2872	0.42	5.0	12	10	10
	2			690	106	2872	0.28	4.7	12	12	11
	1			690	106	2872	0.03	4.5	16	15	12

develop a strong preference for a narrow band of harmonics, and it is reasonable to select the most amplified harmonic as the buckling mode. It is shown there that the mode number initially decreases with time, and after some time the preferred mode does not change appreciably. The buckling mode number predicted in [1], and the corresponding experimental results are listed in Table 1.

Here we assume that the buckling mode develops at an early stage of deformation. For $k = 0.42$ and 0.48 , $(p_2/3)^3 + (q_2/2)^2 > 0$, we use Eqs. (27) and (28). However, for $k = 0.28$ or less, and $(p_2/3)^3 + (q_2/2)^2 < 0$, we employ Eqs. (29) and (30). In this case, there are three real roots for both the maximum initial growth rate of perturbation and the corresponding wave number. In results reported below, we have first solved the cubic algebraic equation by an iterative method for the maximum growth rate of perturbation, and then found the wave number from Eq. (25)₂. The mode numbers predicted by the present theory are listed in the last column of Table 1. Considering the simplicity of our model, the agreement between the predicted and the experimental mode numbers is very good.

3.1.2. Strain rate hardening only materials

Cylindrical shells made of strain-rate sensitive materials such as fully annealed 1015 steel experience dynamic plastic buckling when subjected to large radially inward impulses. A buckling theory, based on resistive moments having a visco-plastic component, is given in [1]. Here we compare the predicted mode number using the perturbation method with experimental results and also with results of Ref. [1]. The variation with time of buckling modes reported in [1] shows that buckling modes do not change substantially after some time. However, at the early stage of deformation, the buckling mode number based on the amplitude

amplification decreases with time but that based on the velocity amplification increases with time.

From Eq. (32) we see that for computing the buckling mode of strain rate hardening only materials, we need the stress level and the value of viscosity. Based on experimental results, Bodner and Symonds [19] have proposed the following empirical relation between the yield stress and the strain rate: $\sigma = \sigma_y[1 + (\dot{\epsilon}/D)^{1/P}]$, where σ_y is the static yield stress, and P and D are empirical constants. For mild steel $\sigma_y = 207$ MPa, $P = 5$ and $D = 40.4 \text{ s}^{-1}$. We have assumed a linear strain-rate hardening relation. Following [1], we take this line to be tangent to the stress–strain curve at the point whose abscissa equals the initial strain rate. Thus, $\mu = \beta\sigma_0 = \sigma_y/PD^{1/P}\dot{\epsilon}_0^{1-1/P}$, where $\dot{\epsilon}_0 = (V_0/R) = (I/\rho hR)$. The intersection of this line with the stress axis gives $\sigma_0 = \sigma_y[1 + (\dot{\epsilon}_0/D)^{1/P}(1 - 1/P)]$. We take $\gamma = \mu/\sigma_0$ and $k = 0.17$. Values of other material and geometric parameters, as well as the buckling mode number computed from Eq. (31) are listed in Table 2. It is evident that the presently computed mode numbers agree well with those observed experimentally.

3.2. Sensitivity of buckling mode to values of material parameters

Cylindrical shells clamped at end faces have zero average axial strain. Short cylindrical shells with no axial restraint from end supports extend axially during their inward radial motion. Long cylindrical shells, even without axial restraints from supports, have axial stresses induced in them by axial inertial forces. For a shell to extend, the material has to be displaced axially away from the central cross section. For sufficiently long shells, zero axial strain conditions are established near the central cross section, whereas near each free end zero axial stress conditions

Table 2
Computed and observed number of half waves for 1015 steel cylindrical shells

Shell number	Radius R (cm)	Thickness h (cm)	Impulse I (Ns/m ²)	Velocity (m/s)	Strain rate (1/s)	σ_0 (MPa)	β (μs)	Half- waves n (Exp.) [1]	Half- waves n (Theo.) [1]	Half- Waves n (Present model)
1a	3.795	0.107	708.9	85.2	2245	576	71.4	26	23	25
1b	3.795	0.107	607.6	73.0	1924	565	82.3	26	22	24
2a	3.815	0.168	1382.3	105.7	2771	592	59.7	19	18	20
2b	3.815	0.168	744.3	56.9	1492	547	104.3	19	15	17
2c	3.815	0.168	744.3	56.9	1492	547	104.3	22	15	17
2d	3.815	0.168	638.0	48.8	1279	537	120.2	22	14	16
2e	3.815	0.168	638.0	48.8	1279	537	120.2	22	14	17
3a	3.780	0.213	2038.2	115.6	3058	600	53.6	13	15	17
3b	3.780	0.214	1514.2	85.9	2273	577	70.6	14	14	16
3c	3.780	0.214	1456.0	82.6	2185	574	73.2	14	14	16
4a	3.835	0.366	3319.6	116.4	3035	599	53.9	9	11	12
4b	3.835	0.366	2096.4	73.5	1917	565	82.8	9	10	11
4c	3.835	0.366	2038.4	71.5	1864	563	84.9	9	10	11
4d	3.835	0.366	1747.1	61.2	1596	552	97.9	9	9	10
4e	3.835	0.366	1513.8	53.1	1385	542	111.8	9	9	10
4f	3.835	0.366	1513.8	53.1	1385	542	111.8	9	9	10

prevail. Thus, for each section of a cylindrical shell, the value of k is essentially fixed throughout its deformations and represents a measure of the axial restraint. At free ends of the shell, $k = 0$, and at the central cross section, the value of k depends on the shell length but approaches zero for very long shells due to axial inertia. Hence it is useful to delineate the influence of k on the buckling mode.

3.2.1. Strain hardening only materials

Values of material and geometric parameters for this parametric study are taken from the first row of Table 1. While conducting the parametric study, only one variable is varied at a time. From the plot of Fig. 2a showing the dependence of the maximum initial growth rate of perturbation and the corresponding number of half waves upon the ratio k , we conclude that they decrease with an increase in the ratio k . For example, the number of half waves decreases from 18 to 14 when k increases from 0 to 0.5 implying thereby that a decrease in the axial restraint increases the wave length of the buckled shape of the shell; this trend agrees with that found in [1]. Fig. 2b depicts the dependence of the maximum initial growth rate of perturbation and the corresponding number of half waves upon the hardening modulus. Both the maximum initial growth rate of perturbation and the corresponding number of half waves decrease monotonically with an increase in the hardening modulus. For example, the number of half waves decreases from 16 to 12 when the hardening modulus increases from 900 to 2500 MPa. Fig. 2(c) exhibiting the dependence of the maximum initial growth rate of perturbation and the corresponding number of half waves upon the applied radial velocity reveals that both the maximum initial growth rate of perturbation and the number of half waves increase dramatically with an increase in the applied radial velocity at first, then increase slowly, and eventually reach a plateau. The number of half waves increases from 7 to 11 with an increase in the applied radial velocity from 9 to 44 m/s; however, the number of half waves increases only from 16 to 17 when the applied radial velocity is increased from 263 to 428 m/s.

3.2.2. Strain rate hardening only materials

We perform the parametric study by taking values of material and geometric parameters from the first row of Table 2. We have plotted in Fig. 3(a)–(c) the dependence of the maximum initial growth rate of perturbation and the corresponding number of half waves upon the axial restraint k , the viscosity, and the radial velocity. As for strain hardening only materials, both the maximum initial growth rate and the corresponding number of half waves decrease with an increase in k . The maximum initial growth rate of perturbation and the corresponding number of half waves decrease rapidly as the material viscosity is increased from its small value, but rather slowly when the viscosity is large to start with. For example, the number of half waves decreases from 48 to 30 when viscosity increases from 1 to 37 μs but decreases from 17 to 14 when the viscosity is

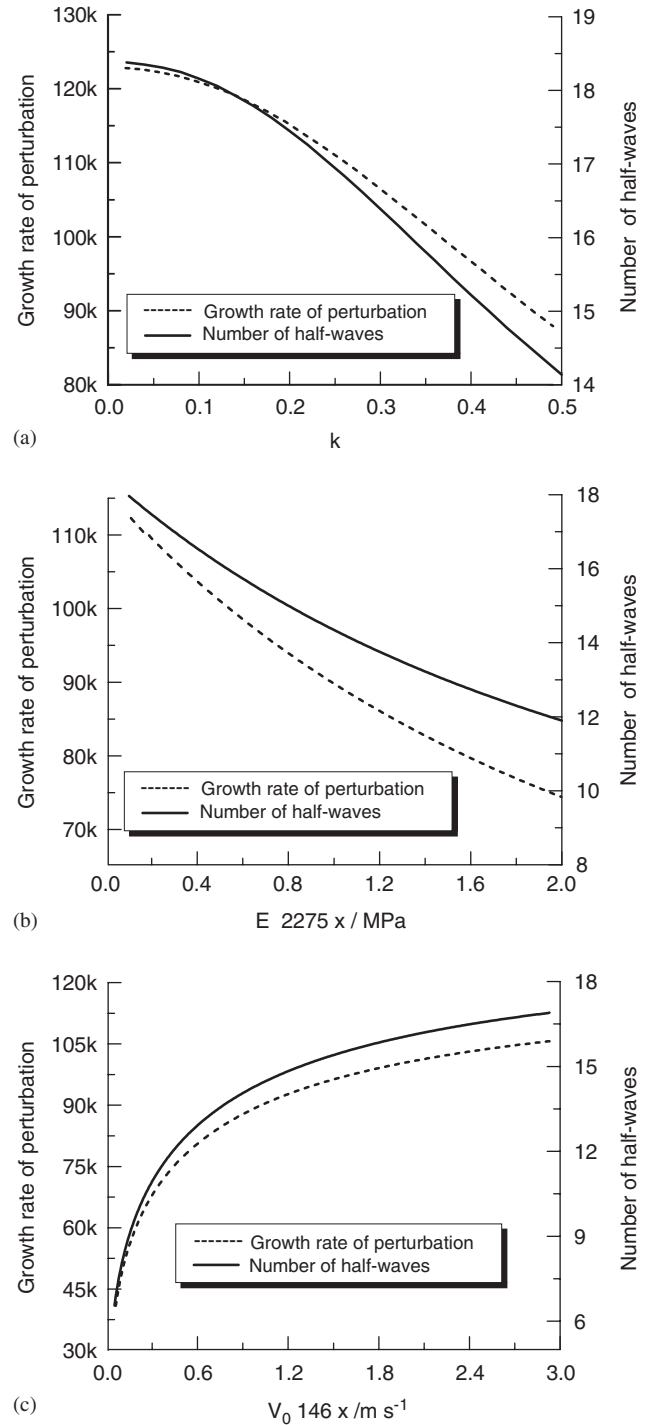


Fig. 2. For strain hardening only materials, dependence of the maximum initial growth rate of perturbation and the corresponding number of half waves upon (a) ratio k , (b) hardening modulus E , and (c) the applied radial velocity V_0 .

increased from 250 to 460 μs . From the plot of Fig. 3(c), we deduce that both the growth rate of perturbation and the corresponding number of half waves increase dramatically with an increase in the applied radial velocity at first, and their rates of increase drop, and their values eventually reach a plateau. For small values of the radial velocity, the

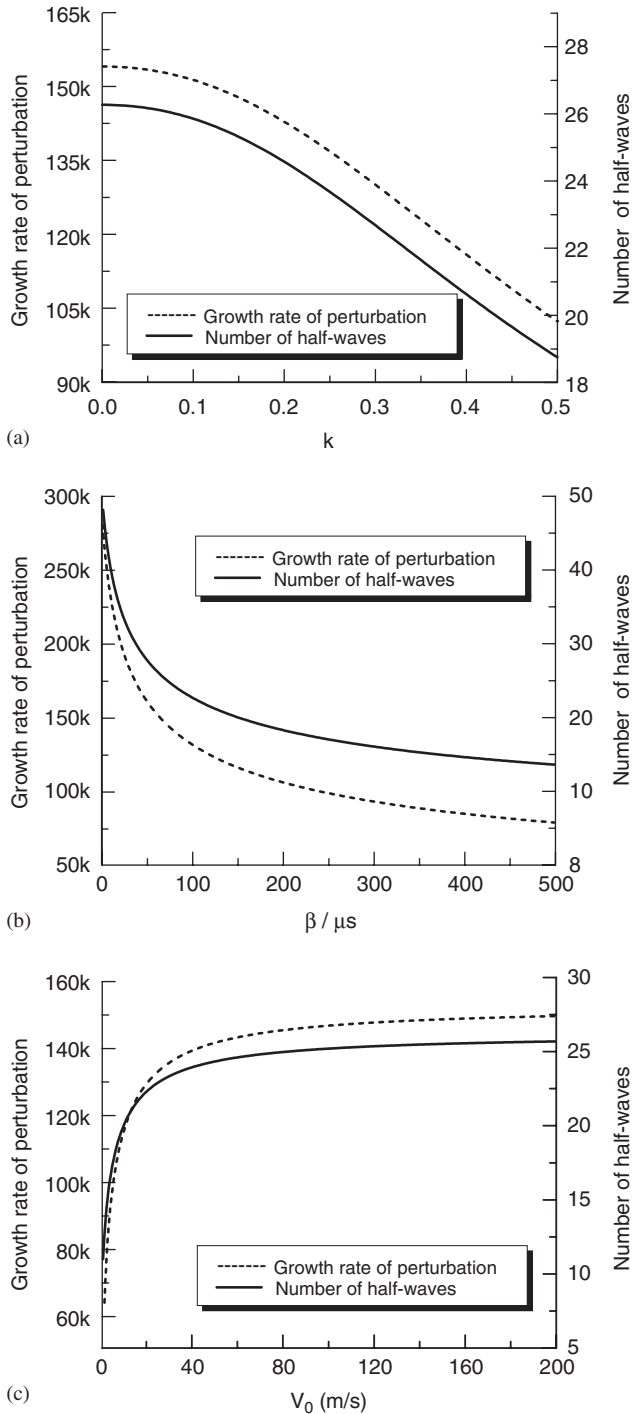


Fig. 3. For only strain rate hardening materials, the dependence of the maximum initial growth rate of perturbation and the corresponding number of half waves upon (a) ratio k , (b) viscosity γ , and (c) the applied radial velocity V_0 .

rate of increase of growth rate of perturbation is higher for strain hardening only materials than that for strain rate hardening only materials. For strain-rate hardening materials, the number of half waves increases from 20 to 24 when the applied radial velocity is increased from 9 to 44 m/s, while the corresponding number of half waves

increases from 24 to 26 when the applied radial velocity increases from 44 to 200 m/s.

4. Remarks

Eqs. (31) and (33) imply that the system is always unstable according to our definition of stability. This is because material elasticity, which stabilizes the system, has been disregarded. Furthermore, the structure becoming unstable does not imply that it cannot sustain additional loads. In fact, a significant portion of the work done by external forces is absorbed during plastic deformations of a structure.

Although buckling initiates at a small strain, in dynamic deformations the initial buckling mode may not prevail since the strain increases rapidly with time, and the preferred buckling mode may change during the deformation process. Hence the final buckled shape will depend on the entire loading history. However, it was observed in [1] that the buckling mode was selected very early in the deformation process. Both the present approach and that employed in [1] give buckled shapes close to those observed experimentally. The present method cannot be used to find energy absorbed during the post-buckling deformations.

At high radial impulsive velocities, the inward displacement of a pre-buckled shell is large, resulting in an appreciable thickening of the shell that diminishes the initial growth of perturbations. This suggests that the stability of the structure improves as it is deformed more severely, and since significant growth of disturbances requires time, at sufficiently high collapse velocities, the buckling may be negligible. However, in our work, the thickening effect has been neglected, and computed buckling loads are highly conservative.

We have considered only bending deformations of the shell, and the effect of axial deformations has been accounted for approximately through the axial constraint factor. For a functionally graded cylinder with material properties varying in the thickness direction, σ_0 , α and β are functions of z . Thus expressions for N_x , N_θ , M_x and M_θ given by Eqs. (15) and (16) will need modification.

The perturbation (22) is invariant when θ is replaced by $\pi - \theta$ implying thereby that not all buckling modes may have been found.

5. Conclusions

The dynamic plastic buckling of a thin linearly strain and strain-rate hardening circular cylindrical shell under radial inward impulse has been investigated. Buckling modes computed on the hypothesis that a shell buckles when the maximum initial growth rate of infinitesimal perturbations superimposed upon the deformed state of the shell is positive and the corresponding wave number of the perturbation determines the buckling mode are found to agree well with experimental findings. The sensitivity of the buckled shape to values of the restraint offered by supports

at the end faces, values of material parameters, and the imposed radial velocity has been delineated. The analysis also provides scaling laws for the wave number of the buckled shape.

Acknowledgements

This work was supported by the ONR Grant N00014-98-1-0300 and N00014-06-1-0567 to Virginia Polytechnic Institute and State University (VPI&SU) with Dr. Y.D.S. Rajapakse as the program manager. Views expressed herein are those of authors and neither of ONR nor of VPI&SU.

References

- [1] Lindberg HE, Florence AL. Dynamic pulse buckling-theory and experiment. Martinus Nijhoff Publishers; 1987.
- [2] Jones N. Structural impact. Cambridge: Cambridge University Press; 1989 Paperback ed., 1997.
- [3] Jones N, Okawa DM. Dynamic plastic buckling of rings and cylindrical shells. *Nuclear Energy and Design* 1976;37:125–47.
- [4] Abrahamson GR, Goodier JN. Dynamic plastic flow buckling of a cylindrical shell from uniform radial impulse. In: Proceedings of fourth US national congress of applied mechanics; 1974. p. 939–50.
- [5] Abrahamson GR, Goodier JN. Dynamic flexural buckling of rods with an axial plastic compression wave. *J Appl Mech* 1966;33:241–7.
- [6] Goodier J.N., Dynamic buckling of rectangular plates and sustained plastic compressive flow, In: Engineering Plasticity, Proceedings International Conference of Plasticity, Cambridge, England, Cambridge: Cambridge University Press, 1968. p. 183–200.
- [7] Florence AL, Goodier JN. Dynamic plastic buckling of cylindrical shells in sustained axial compressive flow. *J Appl Mech* 1968;35(1):80–6.
- [8] Goodier JN, McIvor IK. The elastic cylindrical shell under uniform radial impulse. *J Appl Mech* 1964;31:259–66.
- [9] Lindberg HE. Stress amplification in a ring caused by dynamic instability. *J Appl Mech* 1974;41:392–400.
- [10] Lindberg HE. Buckling of a very thin cylindrical shell due to an impulsive pressure. *J Appl Mech* 1964;31:267–72.
- [11] Anderson DL, Lindberg HE. Dynamic pulse buckling of cylindrical shells under transient radial pressures. *AIAA J* 1968;6:589–98.
- [12] Duffey TA, Warnes RH, Greene JM. Growth of buckling instability during radial collapse of ring. *J Pressure Vessel Technol* 1990;112:145–51.
- [13] Wang R, Ru CQ. An energy criterion for dynamic plastic buckling of circular cylinders under impulsive loading. In: Reid SR, editor. *Metal forming and impact mechanics*. New York: Pergamon Press; 1985. p. 213–23.
- [14] Gu W, Tang W, Liu T. Dynamic pulse buckling of cylindrical shells subjected to external impulsive loading. *J Pressure Vessel Technol* 1996;118:33–7.
- [15] Batra RC, Wei ZG. Dynamic buckling of a thin thermoviscoplastic rectangular plate. *J Thin-Walled Struct* 2005;43:273–90.
- [16] Wei ZG, Yu JL, Batra RC. Dynamic buckling of thin cylindrical shells under axial impact. *Int J Impact Eng* 2005;32:575–92.
- [17] Batra RC, Wei ZG. Shear band spacing in thermoviscoplastic materials. *Int J Impact Eng* 2006;32:947–67.
- [18] Batra RC. Steady state penetration of thermoviscoplastic targets. *Computat Mech* 1988;3:1–12.
- [19] Bodner SR, Symonds PS. Experimental and theoretical investigations of the plastic deformation of cantilever beams subjected to impulsive loading. *J Appl Mech* 1962;29:719–28.